

# IMPACT OF THE SHIP WAVES AND TIDAL FORCES ON THE SEDIMENT RESUSPENSION IN INLAND WATERWAYS

Mainak Chakraborty<sup>1</sup>, V Sriram<sup>2</sup> and K Murali<sup>3</sup>

Ship movement in narrow intertidal waterways generate complex hydrodynamics and sediment resuspension along with tides. In order to investigate the complex hydrodynamics and induced sediment concentration, field measurements were performed at the Falta stretch of the Hooghly river, India. The low frequency primary waves and high frequency secondary waves are dominant in this region as ships navigate in subcritical range due to complex river bathymetry. The time-frequency analysis is a useful tool to separate the ship-generated waves with the tides. The modest performance of the existing empirical models led to the development of the new empirical models for the prediction of ship-generated primary waves. The tides are the dominant factor for the sediment resuspension during the spring period whereas the ship-induced waves are dominant in neap period. The overall contribution of the ship waves on sediment resuspension during the tenure of field measurement was 24.66%.

*Keywords: intertidal waterways; field measurements; sediment resuspension; time-frequency analysis; empirical modelling*

## INTRODUCTION

Inland waterways are one of the natural ecosystem and cheapest mode of transport for bulk materials. The increasing movement of commercial vehicles in the inland waterways has posed a direct threat to the aquatic life and biodiversity of the river. Movement of commercial vehicles in intertidal waterways disturb the natural flow field and create waves along with tidal forcing. The ship-generated waves propagate as a train of waves and reach the river bank. Being one of the main energy inputs in narrow inland waterways, the ship waves could be the governing force behind the change in the cross-sectional profile of the channel. Ship-generated waves have been considered as the major drivers of shoreline erosion (Sorensen 1997) and resuspension of bottom materials, change in biodiversity and loss of aquatic life (Lindholm et al. 2001).

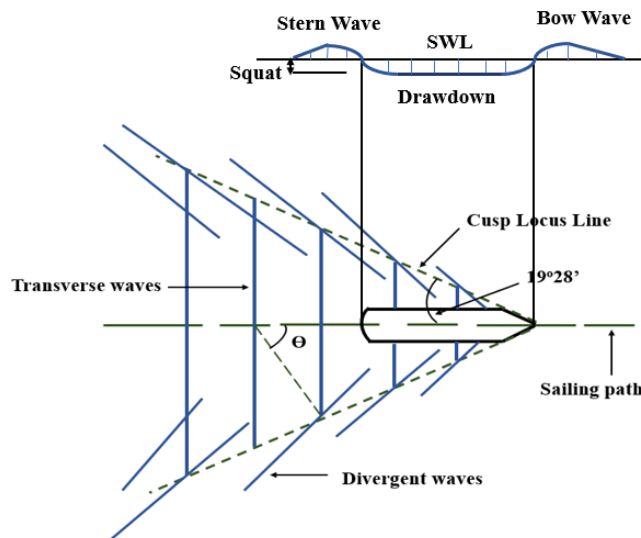


Figure 1. The flow pattern of the typical kelvin waves pattern of ship-generated waves in deep waters. The flow pattern of the depression waves is shown along with the secondary waves. The image is taken from Chakraborty et al. 2022.

<sup>1</sup> Department of Ocean Engineering, Indian Institute of Technology, Madras, Chennai, Tamil Nadu, 600036, India

<sup>2</sup> Department of Ocean Engineering, Indian Institute of Technology, Madras, Chennai, Tamil Nadu, 600036, India

<sup>3</sup> Department of Ocean Engineering, Indian Institute of Technology, Madras, Chennai, Tamil Nadu, 600036, India

As the ship navigates through the water surface, the pressure variation at the air-water interface generates waves in the navigation fairway. Though the wave propagation of the ship waves in deep waters are well documented (Havelock 1908), the study of ship waves in shallow waters are scarce and needs to be explored. In deep waters, a moving ship creates a typical kelvin wake pattern, denoted as divergent and transverse waves (secondary waves) as shown in Fig. 1. The divergent and transverse waves interact among themselves to form cusps, subsequently increasing the wave height, making an angle  $19^{\circ} 28'$  (Chakraborty et al. 2022). On the other hand, in shallow inland waterways, the ship waves are important along with tides and river currents. The main parameter governing the ship waves in shallow waters is depth Froude number given by:

$$Fr_d = \frac{V_{ship}}{\sqrt{gd}} \quad (1)$$

where,  $Fr_d$  is the depth Froude number,  $V_{ship}$  is the ship speed,  $d$  is the water depth and  $g$  is the acceleration due to gravity. In shallow waters, the cardinal parameter depth Froude number is usually less than 1.0 due to limited ship speed. The ship pressure is significantly reduced at the bow and stern and sides of the ship and water level depression occurs at the hull of the ship causing primary waves. The primary waves are mainly dominant in shallow waters and highly insignificant in deep waters. As the primary waves propagate and feel the river bed, the water particle velocity and bottom shear stress increases (Göransson et al. 2013). As the bottom shear stress exceeds the threshold value, sediment particles are resuspended from the bed and carried downstream with the river currents. On the other hand, the significance of secondary waves is pronounced when the depth Froude number varies between 0.5 to 1.0. The increase in the depth Froude number causes the cusp locus angle to increase from  $19^{\circ} 28'$  to  $90^{\circ}$ . The divergent and transverse waves interact among themselves forming leading wave profile (Sorensen and Weggel 1984).

As the ship waves propagate towards the river banks, they feel the river bed due to limited water depth. Shorelines are important natural infrastructures along our coasts since they provide ecosystem services in the form of erosion mitigation, biological diversity, recreational and aesthetic values (Barbier et al. 2011). The major impact of the ship-generated waves has been witnessed in the river bank and shoal areas due to the wave-breaking process (Fleit et al. 2019). The shallow water flows cause high bed shear stress and resuspension of fine sediment particles. The resuspended sediment particles are transported with the river currents and deposited downstream, thus increasing the overall dredging cost of the waterways (Gelinas et al. 2013). Though the individual effect of ship waves on sediment re-suspension was reported by Osborne and Boak 1999, the movement of ship traffic in the intertidal environment of inland waterways are unexplored. It is crucial to identify which component (primary and secondary) of the wave train is comprised of higher erosional capacity. The extraction of the ship waves and contribution of the individual ship movement in the sediment processes, particularly in the intertidal environment is cumbersome and never reported to our knowledge.

Out of the 111 national waterways in India, 13 waterways are operational for shipping activities as per the Ministry of Ports, Shipping and Waterways, India. The Ganga-Bhagirathi-Hooghly river (National Waterway 1) is the longest river in India connecting Prayagraj in Uttar Pradesh to Haldia in West Bengal. The national waterway 1 experienced a ship traffic of 3518 deep-draft vessels in the year 2019-2020 as it is the home to two major ports in India viz. Syama Prasad Mookerjee Port (SMP) and Haldia Dock Complex (HDC). The vessels navigating the river have a length range of 105 m to 155 m, a width of 18 m to 25 m and a draft from 4 m to 7 m. The speed of vessels in the river varies between 6 to 13 knots, depending on the river geometry.

The present study aims to conduct field measurements in the Falta region of the Hooghly River, India to analyze ship generated waves, tides and sediment re-suspension. The extraction of the ship waves from the collected water surface elevation was carried out by time frequency method and erosive nature of various wave components are reported. Further, the influence of the individual ship waves along with tidal forcing in the sediment re-suspension will be reported. Based on this, we propose new empirical relationship for the evaluation of the primary and secondary waves from the measured data set which can be employed in the designing of river bank protection works.

## MATERIALS AND METHODS

### Study Area

The National Waterway 1 connects three states out of which the Hooghly river segment in West Bengal is the busiest one due to the presence of two major ports, connecting the eastern part of India to the rest of the world. The Hooghly river starts from Nabadwip in West Bengal and gets truncated at the Bay of Bengal near the Sagar islands. The river is generally known as Bhagirathi river upstream of Nabadwip. The overview of the study location is shown in Fig. 2. The field measurements were carried out in the Falta jetty (see point A, Fig. 2) on the Hooghly river, West Bengal, India. The latitude and

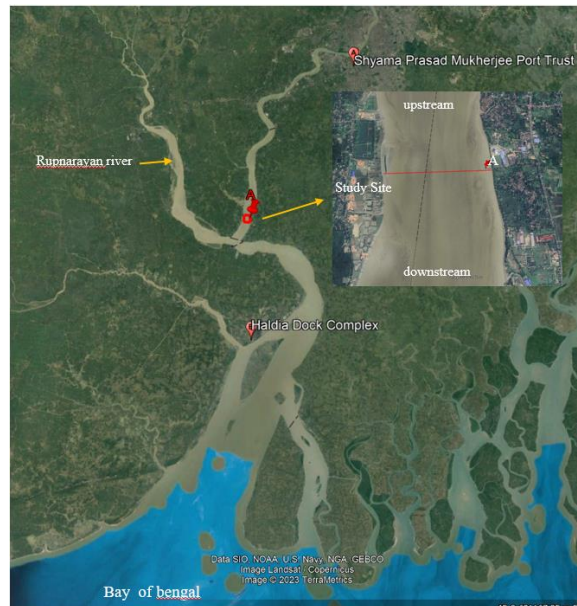


**Figure 2.** The overview of the study site with SMP at the upstream and HDC at the downstream. The enlarged view of the study site (denoted by red box) is shown on the right side of the figure. The measurement point A ( $22^{\circ}15'17.57''\text{N}$ ,  $88^{\circ}5'16.19''\text{E}$ ) is located on the Falta jetty which is 76.5 km from the left bank.

longitude of the measurement point is  $22^{\circ}15'17.57''\text{N}$  and  $88^{\circ}5'16.19''\text{E}$  respectively. The river forms a tributary, Rupnarayan river, 5 km downstream of the measurement station. The river experiences fresh water discharge from the upstream and saline water is infused from the downstream along with tidal forcing. The effect of salinity is minimal at our study location and the water is mainly fresh water. The normal freshwater discharge from June to October is about  $3000\text{ m}^3/\text{s}$  and from November to May is around  $1000\text{ m}^3/\text{s}$  (Sadhuram et al. 2005). The field measurements were performed for 11 days, starting from 23<sup>rd</sup> August 2021 and ending on 2<sup>nd</sup> September 2021. The tidal variations in the region are semi-diurnal in nature with tidal currents ranging between 1 m/s to 1.5 m/s. The river often experiences tidal bores at certain stretches due to limited water depth. More details about the study site can be found at (Chakraborty et al. 2022).

In context to the sediment variability in the Hooghly river, sampling studies show that suspended sediments could vary to a great extent spatially. Most of the sediments are non-cohesive sand number of components of different grain sizes where individual particles are assumed to be spherical, non-cohesive having density of  $2650\text{ kg/m}^3$  (Arora and Bhaskaran 2012). The Hooghly estuary is highly dynamic in terms of its suspended load. It has an annual runoff of approximately  $493\text{ km}^3$  and carry about  $616 \times 10^6\text{ t}$  of suspended solids to the estuarine mouth (Qasim et al. 1988). It is considered the second major river in the world in context of suspended load contributing sediments to the Bengal deltaic fan considered the largest deep sea fan in the world (Lisitzin 1972).

### Field Measurements

The field measurements were performed on spring and neap tide period. The data collected from 23<sup>rd</sup> August to 27<sup>th</sup> August was during the spring tide, while from 28<sup>th</sup> August to 2<sup>nd</sup> September was during the neap tide. The mean discharge during this period was  $2590\text{ m}^3/\text{s}$  (Chakraborty et al. 2022).

The continuous data of the water surface elevation due to tides and ship-generated waves were measured using ultrasonic recorder (LOG aLevel®, General Acoustics) with sampling frequency of 5 Hz. The instrument was placed 1 m outside the jetty at measurement point A. The river velocity and backscattering intensity data was collected using horizontally looking Acoustic Doppler Current Profiler (ADCP) (Channelmaster, Teledyne). This was mounted 4.5 m above the river bed as shown in Fig. 3(b). The ADCP was mounted at this location to neglect the effect from river bed and effectively capture the ship wave effects. The ADCP sampled at 2 Hz and averaged data over 5 minutes are considered to reduce the uncertainties due to turbulence. The ADCP data was collected only during the

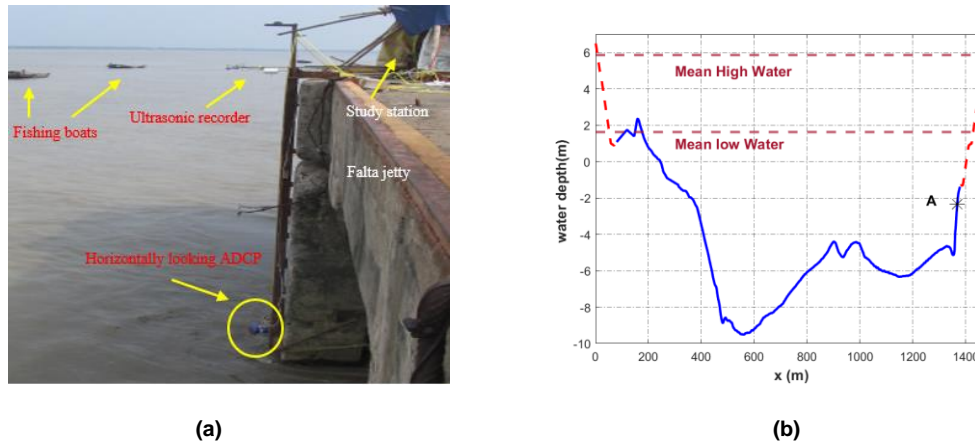


**Figure 3. (a) Setup of ultrasonic recorder and horizontal looking ADCP. The instruments are mounted on the Falta jetty. Adequate spacing between the two instruments is maintained to neglect the interference of one instrument with the other. The image is captured during low tide. (b) Cross-sectional profile of the river near Falta jetty. The point A denotes the measurement location of ship waves and tidal forcing along with river currents. The red dashed line indicates the approximate river bank profile which submerges during high tide and emerges out during low tide.**

day time (as there is no ship movement during night time) until the ADCP came out of water. ADCP instruments transmit acoustic signals to the water column and hit underwater objects like suspended sediments (Simmonds and MacLennan, 2005). The acoustic signals from the sediments were backscattered to the ADCP and is termed as backscattering intensity. The SSC was estimated from this backscattering intensity by means of sonar principle. The backscattering intensity was calibrated using field measured SSC (measured using Niskin Sampler of 2.5 litres). The calibration equation obtained from the linear regression analysis was applied to the present study.

The bathymetry data was obtained by using an echo sounder and DGPS mounted on the launch vessel. The water depth in the study area varies from +2.35 m to -9.35 m, as shown in Fig. 3(b) with respect to the Chart Datum (CD), which is 2.82 m below the mean sea level (MSL). The study location has varying tides during the period of measurements. Hence, in the present study, the CD is referred to as 0 levels; any value above the CD level is positive, that is, the land area while the value below the CD level is water level denoted by negative values. Therefore, positive and negative values are used to differentiate between land area and water depth because of the tide variations dominant in that area. More details about the field measurement and data analysis procedure are reported in Chakraborty et al. 2022.

### Spectrogram Analysis

Ship movement at shallow intertidal waterways generate both primary and secondary waves (see Fig. 1) as they propagate with limited ship speed and varying depth Froude number between 0.2 to 1. As these waves are comprised of linear and non-linear components (Didenkulova et al. 2013), appropriate methods should be deployed to separate these waves from the tidal forcing. Ships traveling at high velocity generate non-stationary components. Under these complex conditions, the traditional stationary process (ergodic) and statistical methods fail to characterize the ship waves and extraction of the ship waves from the tidal fluctuations is complex. In contrast with marine and lacustrine conditions, where it is a common practice to characterize longer time periods (hours, days) with a stationary wave spectrum, ship-induced wave trains usually change their characteristics under much smaller time scales

(minutes, seconds) (Fleit et al. 2019). Therefore, using time-frequency analysis could be a valuable tool for identifying ship waves. Owing to the finite spatial extensions (Torsvik et al. 2009), transient nature and short timescale, the ship waves appear as chirp signals (frequency increasing with time) in the time domain. Therefore, by applying spectrogram analysis to the measured time series, the ship wakes were identified by monotonically increasing peak frequency, where the energy content was highest.

The spectrogram study is a reliable decomposition of the wave signal in the time-frequency domain based on the short-term Fourier transform. The analysis was carried out in MATLAB software with a Hamming window of 180 seconds and a window overlap of 170 seconds. The results are reported in a time-frequency heat map of frequency against time with colour intensity of  $\log_{10}(\text{PSD})$ , where PSD is the power spectral density.

## RESULTS AND DISCUSSION

### Ship-generated Waves

The most common navigation vessels could be divided into two types displacement and planing vessels. The present study area mainly experiences deep-draft large commercial displacement vessels navigating both upstream and downstream during high tide only. The ships navigate during the high tide alone due to limited water depth availability in the study domain. The field measurement campaign collected 24 ship data and analysis was carried out. The list of the ships navigating through the study domain are listed in Chakraborty et al. 2022. The flow of ship traffic was listed in a datasheet containing the ship name, time of arrival and departure from Falta jetty along with the real time ship movement direction during the period of survey and important ship parameters were obtained. The time-frequency analysis of the raw data revealed that ship waves appear as chirp signal due to its transient nature (Sheremet et al., 2012) and could be easily identified from the raw data. For each ship passage, the water surface elevations were extracted four minutes before and up to ten minutes after the passage of the ship and subtracted over the mean value. The time frequency analysis of the extracted data confirmed the presence of ship waves. The frequency difference between ship-generated waves and tides was the key factor to separate them. The comparison of the spectrogram analysis of the water surface elevation for one such ship MTT Senari and no ship period is reported in Fig. 4. The time frequency analysis of the extracted ship wave data revealed the energy contained in different wave components (see Fig 4(a)). Whereas, there is a strong absence of high energy during no ship activity period between 9:40 hrs to 9:55 hrs as shown in Fig. 4(b). The above methodology confirms the effective separation of the ship waves with the tides.

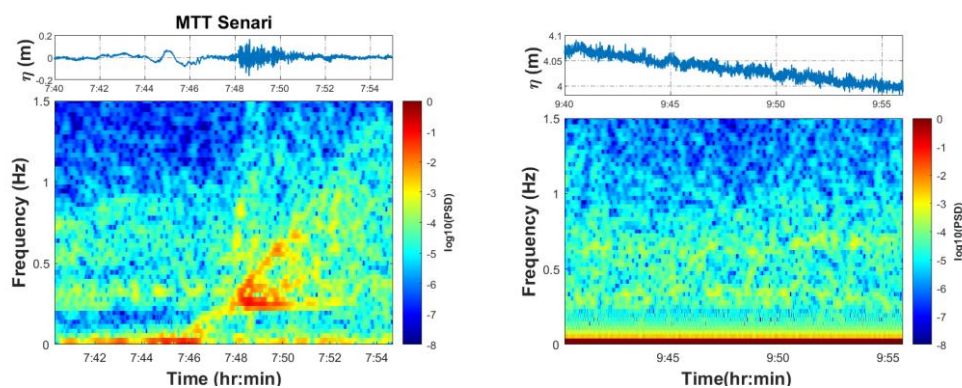


**Figure 4. (a) Spectrogram plot of the ship MTT Senari after extraction from the raw data comprising of tides and ship waves. (b) Spectrogram plot of water surface elevation during no ship activity period. The water surface elevation for the present study was measured on 2<sup>nd</sup> September 2021.**

The ship MTT Senari navigated with a depth Froude number of 0.718. Therefore, the ship waves consist of two sets of higher energy, one is the primary wave (lower frequency) and other is secondary waves consisting of a sliding frequency mode caused by divergent waves and constant frequency mode for the transverse waves (Fig. 4(a)). The highest energy is noticed at the fold, where divergent waves meet the transverse waves. The divergent waves are short-lived and display high non-linearity as they originated at a frequency of 0.25 Hz and evolved to a higher frequency of 0.7 Hz. On the other hand, the transverse waves maintained a constant frequency at 0.25 Hz and are noticed for a long time after

ship passage. The lower frequency primary waves exhibit high energy and are detrimental in river bank and bed erosion in inland waterways due to lack of sufficient water depth. Therefore, determination of the primary and secondary waves is useful to understand the characteristics of ship waves.

The enlarged view of the water surface elevation generated due to the movement of the ship MTT Senari is displayed in Fig. 5(a). The water profile shows an initial surge and significant depression between 7:40 hrs and 7:46 hrs, termed as primary waves or drawdown. The waves recorded after the primary waves between 7:48 hrs and 7:51 hrs attains a peak after 4-5 waves and gradually decreases. These waves are termed as divergent waves. The remaining set of waves are transverse waves. The divergent and transverse waves are cumulatively termed as secondary waves. The low pass filtering at cut-off frequency of 0.03 Hz separates the primary wave with the secondary waves.

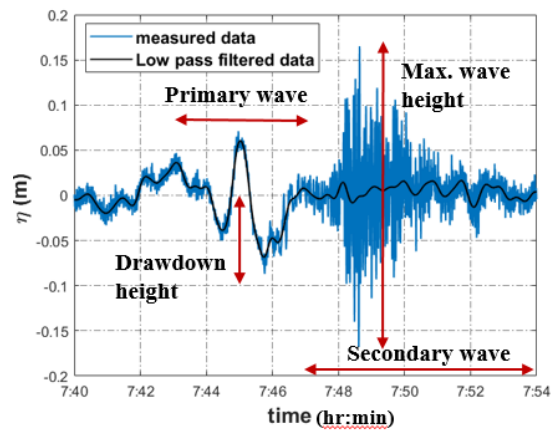


**Figure 5. Spectrogram plot of the ship MTT Senari after extraction from the raw data comprising of tides and ship waves.**

The energy analysis of the water surface elevation of the ship MTT Senari revealed that the total energy contained in the wake train is 0.917 J. Out of which, the maximum contribution came from the divergent wave group comprising of 48% of the total energy. This was followed by the primary waves comprising of 38% of the total energy and the least contribution came from the transverse wave group with a share of 14% of the total energy. Therefore, determination of the primary and secondary wave height is useful to understand the erosive potential of the wave train.

#### **Empirical Modelling of Ship Waves**

The primary wave height or drawdown height was estimated as the vertical distance between the mean water level and the minimum water level as displayed in Fig 5. The minimum drawdown in the entire study was 0.02 m, and the maximum drawdown was 0.11 m. The large river width (1363 m) in the study area is the primary reason behind generating a relatively minor drawdown height than the maximum wave height of the secondary waves. The correlation study between the crucial parameters and measured drawdown revealed that the highest correlation was for ship dimensions, mainly the ship length and ship blockage ratio (ratio between the submerged area of the ship to the cross-sectional river area). Interestingly, it was found that drawdown height is not dependent on the ship speed and depth Froude number, which is considered a key parameter for water surface fluctuations in restricted waterways (Briggs et al. 2009).

The measurement of the maximum wave height from the divergent waves is the key to determining the destructive nature of the wave group. The maximum wave height is calculated by the zero up-crossing methods and is the vertical distance between the maximum trough and the corresponding maximum crest of the divergent wave group (Chakraborty et al. 2022). The maximum wave height varied between 22 cm to 73.2 cm. The primary and secondary waves are poorly correlated with each other. Therefore, the physics and parameters involving the variation in the maximum wave height in the wave train are different and should be analyzed. The correlation study between the maximum wave height and cardinal ship parameters revealed that the secondary ship waves are mainly dependent on ship speed and depth based Froude number (Eq. 1).

The empirical models used in literature are mainly derived based on the modeled scaled results of tug boats and barges on a uniform bathymetry. The detailed analysis of the empirical models used in the

determination of primary and secondary waves are reported in Chakraborty et al. 2022. The existing empirical models are highly site-specific. They could not address the non-linearity associated with the ship waves propagating in the non-uniform bathymetry of the Hooghly river. Therefore, based on correlation study and regression analysis, the authors developed two new empirical equations for the prediction of drawdown height ( $s_d$ ) (Eq.2) and maximum wave height ( $H_m$ ) (Eq. 3) of the divergent wave group.

They are as follows:

$$s_d = \left(\frac{L}{d}\right)^{0.6} \left(\frac{A_s}{A_c}\right)^{1.3} \frac{U_{ship}^2}{2g} \quad (2)$$

where,  $L$  is the length of the ship,  $d$  is the water depth at the measurement location during the time of ship passage,  $A_s$  is the submerged cross-section of the ship,  $A_c$  is the cross-sectional area of the navigable channel,  $U_{ship}$  is the ship velocity and  $g$  is the acceleration due to gravity.

$$H_m = md \left(\frac{x}{d}\right)^{-0.33} Fr_d^{3.2} \quad (3)$$

where,  $x$  is the shortest distance from the sailing path to the measurement point,  $Fr_d$  is the depth-based Froude Number. The term  $m$  incorporates the bow geometry of the ship, expressed as  $m = \frac{B}{L_e}$ , where  $B$  is the beam of the ship and  $L_e$  is the entranced length.

The performance of the derived empirical models with the measured data is reported in Fig. 6.

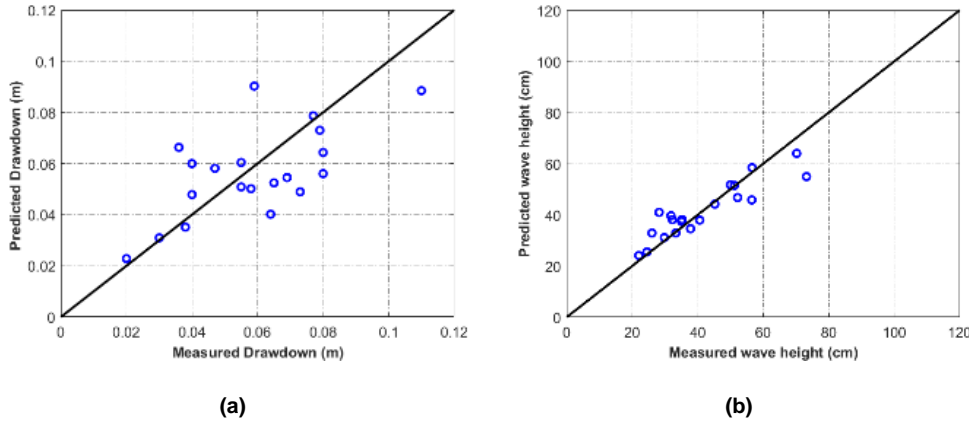


**Figure 6. Comparison of the (a) predicted drawdown height (left figure) and (b) the maximum wave height of the divergent wave group using newly developed empirical equations with the measured data. The black solid line indicates the perfect match.  $R^2$  value for  $s_d$  and  $H_m$  is 0.43 and 0.83 respectively with rms error of 0.26 and 0.15.**

The co-efficient of determination ( $R^2$ ) for  $s_d$  and  $H_m$  are 0.43 and 0.83 respectively, whereas the root mean square error value are 0.26 and 0.15 respectively. The correlation between predicted and measured  $s_d$  and  $H_m$  are 0.65 and 0.91 respectively. It is worthy of mention that in Eq. 2,  $L/B$  also correlated well with the measured  $s_d$  but  $B$  is directly proportional to  $s_d$  so  $B$  cannot be in the denominator, so the dimensionless term  $L/B$  was discarded. Moreover, in Eq. 3, the incorporation of the term  $m$  addressed the effects from the hull of the ship, which was not present in the empirical models found in literature. The above empirical models are developed based on field measurement data in the Hooghly river. Therefore, proper calibration and detailed study must be performed before execution in other waterways.

**Influence of Ship Waves and Tides on Sediment Resuspension**

In the previous section, we have identified that time-frequency analysis is an effective tool in identifying the ship-generated waves and separate them from the tides. Since, the time-series of the water surface elevation due to ship-generated waves has been identified, this makes our task easy to analyze the sediment resuspension due to the concerned ship. The backscattering echo intensity at the

exact same time of the ship passage through our study domain is identified and applied to the calibration equation. The suspended sediment concentration (ssc) obtained by this process contains the influence of tides along with the ship-generated waves.

The influence of the individual ship movement on ssc in a tidal dominated river is difficult to assess due to ever changing river conditions. However, in our study domain, the ships navigate in close intervals during the high tide alone due to lack of adequate draft. Therefore, there is not much variation in the river conditions during ship passage. Contrary to tidal waves, flow velocities under ship waves can increase by order of magnitude within seconds, resulting in a less gradual, almost instantaneous increase in ssc. Moreover, the ssc only increases for relatively short periods (per wave event), in order of minutes after a passing vessel, as waves attenuate much faster (Bauer et al. 2002, Smarts et al. 1985). Therefore, by applying a moving average filter to the ssc data, one could successfully identify the individual contribution of a particular ship. The results of the ssc data obtained for the ship MTT Senari is reported in Fig. 7.

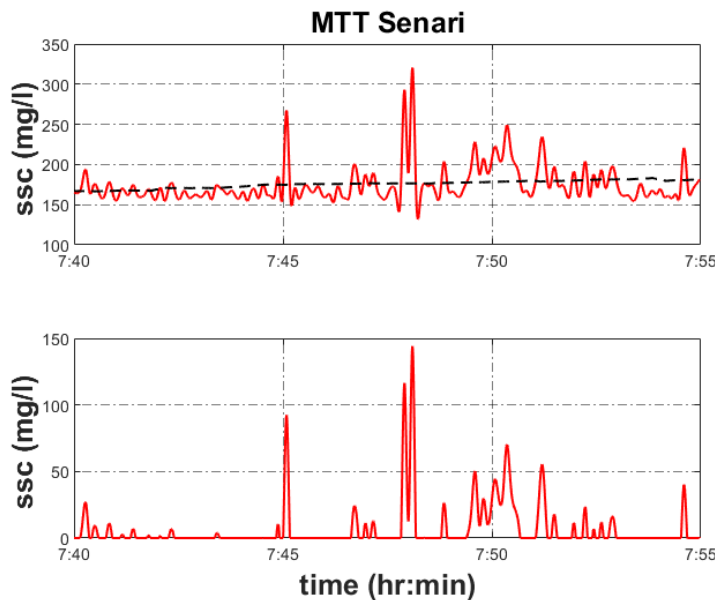


**Figure 7. Top figure shows the measured ssc during the passage of the ship MTT Senari along with tidal influence. The bottom figure shows the contribution of the ship MTT Senari alone after applying a moving average filter displayed by dashed black line in top figure.**

Fig. 7 reveals that the maximum ssc due to the ship MTT Senari is observed between 7:45 hrs and 7:50 hrs. This is the same time frame where we observed the maximum intensity in the spectrogram plot Fig. 4(a). Therefore, we have correctly estimated the ssc generated due to the propagation of the ship MTT Senari. The maximum ssc contribution due to primary and secondary waves are 92.28 mg/l and 144.6 mg/l respectively. Therefore, both primary and secondary waves are detrimental for the river bank and bed erosion in inland waterways. Similar operation was performed to the entire data set and ssc contribution of all the ships were evaluated.

The ship-generated waves and tides are the main drivers of suspended sediments in intertidal inland waterways. The influence of the tides and ship-generated waves on the ssc contribution in the National Waterway 1 of India is discussed here. There is a clear difference in the sediment flux between the spring tide period (25<sup>th</sup> August – 27<sup>th</sup> August 2021) and neap tide period (28<sup>th</sup> August- 02<sup>nd</sup> September 2021). The results on 1<sup>st</sup> September 2021 were not obtained due to instrument failure. It was found that the river experiences more sediment re-suspension during the spring period compared to the neap period. The ssc due to flood and ebb currents were 111.62% and 36.6% greater in the spring period than the neap period. High river currents and larger variation in the amplitude during the high and low tide during the spring period induces greater ssc and the influence of the ship waves on the ssc is suppressed. The river experiences tidal bores at certain stretches of the channel where water depth is relatively low.



The Hooghly river experiences semi-diurnal tidal variation with the ship movement occurring during the high tide time. There is a phase in the river when the river currents are almost 0 m/s and there is no influence of flood currents, ebb currents and ship-generated hydrodynamics. This is the calm water phase and ssc during this time is termed as background ssc or calm period ssc. Now in order to compare the influence of tides and ships on ssc, the calm water ssc is subtracted from the ambient raw data to analyze the individual effect of all the phenomenon. The comparison of the sediment resuspension due to flood currents, ebb currents, ship-induced currents and calm water period is shown in Fig. 8. As the field measurements were carried out during spring and neap periods, the comparative analysis is performed separately for both the phases.

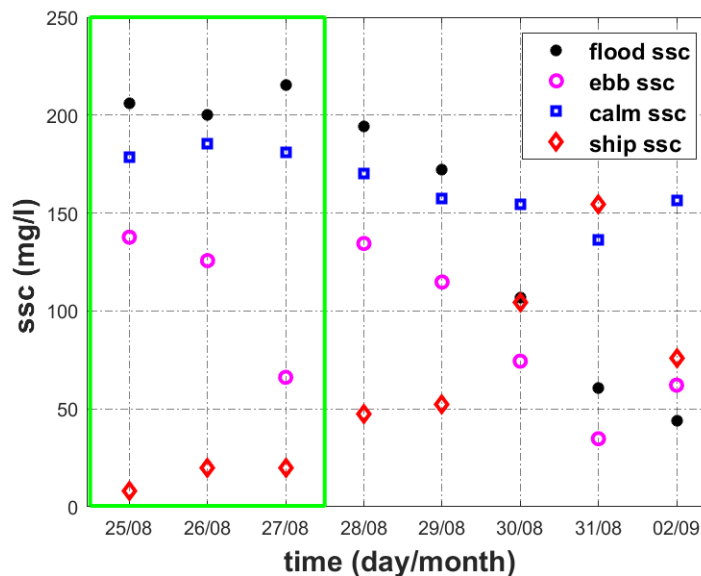


Figure 8. Day wise comparative plot of the ssc due to the flood currents, ebb currents, calm water period and ship-induced currents. The green box shows the data during spring period.

Fig. 8 confirmed that the sediment resuspension due to flood currents are maximum during the spring period whereas, the ship-induced hydrodynamics are the dominant factor for sediment resuspension in the neap period. Comparative analysis revealed that ssc contribution of the ship waves are only 7.71% and 17.34 % with respect to the ssc contribution of flood and ebb currents respectively during the spring period. On the other hand, the ship-induced ssc contributed 115.97% and 157.42% in the neap period with respect to the ssc contribution of flood and ebb currents. The overall contribution of the ship waves during the tenure of the field measurements with respect to the background ssc during the calm period is 24.66%. Though tidal forcing is the significant contributor of ssc in inter-tidal waterways, the contribution of ship waves is quite significant and should be considered to maintain a sustainable waterway.

## SUMMARY AND CONCLUSIONS

The present study investigated the influence of ship-generated waves and tides on the sediment resuspension by means of field measurements. The ships navigate in subcritical range at the study domain leading to the generation of both primary and secondary waves. Time-frequency analysis is an effective tool to separate the ship-induced waves and tides. The instantaneous increase in ssc due to ship-generated waves was analyzed by using a moving average filter.

The analysis of the primary waves revealed that they are highly correlated to the ship length and blockage ratio. On the other hand, the secondary waves are correlated to the ship-speed and depth Froude number. The prediction of the primary and secondary wave height gives a direct understanding of the erosive potential of the wake train. The modest performance of the existing empirical models led to the development of new empirical model for the prediction of primary and secondary waves. The correlation coefficient between the measured and predicted data was 0.65 and 0.91 for the primary and secondary waves respectively.

The comparative analysis of the ssc due to ship-generated waves and tides revealed that the tidal forcing is more pronounced during the spring period. Large variation in amplitude of the water surface elevation and high river currents during the spring period suppressed the influence of ship-generated waves. On the other hand, the ship-induced waves are the dominant factor during the neap period. Therefore, the combined effect of tides and ship-generated waves are significant drivers of sediment transport in intertidal waterways.

It is worthy of mention that ship traffic and seasonal variability are important parameters in the evaluation of ssc. As our study was conducted during the monsoon period, the effect of ship waves may be somewhat suppressed due to upstream discharge. Our study for a limited period in the Hooghly River revealed that ship waves contribute 24.66% on the total sediment re-suspension. Therefore, large scale implication of ship waves will adversely impact the river stability and biodiversity of the aquatic life.

#### ACKNOWLEDGMENTS

The authors would like to acknowledge National Technology Centre for Ports, Waterways and Coasts (technical wing of the Ministry of Shipping, India) for supporting the study, which is under the project “Assessment tool for assessing the impact of Ship/Boat Wake Waves on the banks and protection measures for Inland National Waterways”. The authors would like to thank the Ocean Engineering Department project staff, IIT Madras, for their valuable contribution to the field survey. The authors would like to appreciate the constant support and cooperation of the Hydraulic Study Department of Syama Prasad Mookerjee Port. The authors would like to thank the Department of Commerce, Government of India, for providing permission to access the Falta jetty to carry out the field investigations.

#### REFERENCES

- Barbier, E.B., Hacker, S.D., Kennedy, C., Koch, E.W., Stier, A.C., and Silliman, B.R. 2011. The value of estuarine and coastal ecosystem services, *Ecological Monographs*, 81: 169-193.
- Bauer, B., Lorang, M., Sherman, D. 2002. Estimating boat-wake-induced levee erosion using sediment suspension measurements. *Journal of Waterway Port Coastal and Ocean Engineering*, ASCE, 128.
- Briggs, M., Vantorre, M., Uliczka, K., and Debailon, P. 2009. Prediction of squat for under keel clearance. in handbook of coastal and ocean engineering; (Chapter 26 ed.). Los Angeles, CA, USA: *WORLD SCIENTIFIC*.
- Chitra Arora, and Prasad K. Bhaskaran. 2012. Parameterization of bottom friction under combined wave-tide action in the Hooghly estuary, India, *Ocean Engineering*, Volume 43, pp 43-55, ISSN 0029-8018.
- Chitra Arora, and Prasad K. Bhaskaran. 2013. Numerical Modeling of Suspended Sediment Concentration and Its Validation for the Hooghly Estuary, India, *Coastal Engineering Journal*, 55:2, 1350006-1-1350006-23.
- Didenkulova, I., Sheremet, A., Torsvik, T., and Soomere, T. 2013. Characteristic properties of different vessel wake signals, *J. of Coastal Research*, pp. 213–21.
- Fleit, G, Baranya, S, Krámer, T, Bihs, H., and Józsa, J. A. 2019. Practical framework to assess the hydrodynamic impact of ship waves on river banks. *River Res Applic*, 35: 1428– 1442.
- Göransson, G., Larson, M., and Althage, J. 2013. Ship-generated waves and induced turbidity in the Göta Älv River in Sweden, *Journal of Waterway Port Coastal and Ocean Engineering*, 140.
- Havelock, T. H. 1908. The propagation of groups of waves in dispersive media, with application to waves on water produced by a travelling disturbance, *Proceedings of The Royal Society A: Mathematical, Physical and Engineering Sciences*, 81, 398-430.
- Lindholm, T., Svartström, M., and Spoof, L. *et al.* 2001. Effects of ship traffic on archipelago waters off the Långnäs harbor in Åland, SW Finland, *Hydrobiologia* 444, 217–225.
- Lisitzin, A.P. 1972. Sedimentation in the World Ocean. *Society of Economic Paleontologist and Mineralogists*. Special publication No. 17, 218 pp.
- Mainak Chakraborty, V. Sriram, and K. Murali. 2022. Field measurement and analysis of ship generated waves in Hooghly river, India, *Applied Ocean Research*, Volume 128, 103337, ISSN 0141-1187.
- Morgan Gelinias, Henry Bokuniewicz, John Rapaglia, Kamazima, and M.M. Lwiza. 2013. Sediment Resuspension by Ship Wakes in the Venice Lagoon, *Journal of Coastal Research*, 29(1), 8-17.

- Qasim, S.Z., Sengupta, R., and Kureishy, T.W. 1988. Pollution of the seas around India. *Proc. Ind. Acad. Sci. (Anim. Sci.)*, 97, 117–131.
- Sadhuram, Y., Vvss, S., Murthy, T., and Rao, B. 2005. Seasonal variability of physico-chemical characteristics of the Haldia channel of Hooghly estuary, India. *Journal of Earth System Science*, 114, 37–49.
- Simmonds, J., and MacLennan, D. 2005. *Fisheries Acoustics: Theory and Practice*. New Jersey, USA: Blackwell Publishing Ltd.
- Sheremet, A., Gravois, U., and Tian, M., 2012. Boat-wake statistics at Jensen beach, Florida. *Journal of Waterway, Port, Coastal and Ocean Engineering*, 139, 286–294.
- Smarts, M.M., Radar, R.R., Nielsen, D.N., and Claflin, T.O. 1985: The effect of commercial and recreational traffic on the resuspension of sediment in navigation pool of the upper Mississippi river. *Hydrobiologia* 126, 263–274.
- Sorensen, R. M. 1997. Prediction of vessel-generated waves with reference to vessels common to the upper mississippi river system, ENV report 4; *prepared for U.S. Army Engineer District*, Rock Island, U.S. Army Engineer District, St. Louis, U.S. Army Engineer District.
- Sorensen, R. M., and Weggel, J. R. 1984. Development of ship wave design information, *Coastal Engineering Proceedings*, 1 (19), 216.
- Torsvik, T., I, D., T, S., and Parnell, K. 2009. Variability in spatial patterns of long nonlinear waves from fast ferries in Tallinn Bay. *Nonlinear Processes in Geophysics*.
- Osborne, P.D., and Boak, E.H. 1999. Sediment suspension and morphological response under vessel-generated wave groups: Torpedo bay Auckland, New Zealand. *Journal of Coastal Research* 15, 388–398.